

199001158 N90-26774

592689

LIQUID-VAPOR EQUILIBRIUM OF MULTICOMPONENT CRYOGENIC SYSTEMS

2915

W. REID THOMPSON,* JORGE C. G. CALADO** AND JOHN A. ZOLLWEG†

*Laboratory for Planetary Studies, Space Sciences Bldg., Cornell Univ., Ithaca, NY 14853

**Complexo I, Instituto Superior Técnico, 1096 Lisboa, Portugal

†School of Chemical Engineering, Olin Hall, Cornell Univ., Ithaca, NY 14853

ABSTRACT

Liquid-vapor and solid-vapor equilibria at low to moderate pressures and low temperatures are important in many solar system environments, including the surface and clouds of Titan, the clouds of Uranus and Neptune, and the surfaces of Mars and Triton. The familiar cases of ideal behavior ($p_i = X_i p_i^o$, where p_i is the vapor pressure of a species present at mol fraction X_i in a condensate, and p_i^o is its vapor pressure in the pure state), and Henry's law [$X_i = p_i/K_H$, where K_H is the Henry's law constant for a given solute (gas) and solvent (liquid)] are limiting cases of a general thermodynamic representation for the vapor pressure of each component in a homogeneous multicomponent system: $p_i = \gamma_i X_i p_i^o$, where γ_i is the activity coefficient. The fundamental connections of laboratory measurements to thermodynamic models are through the Gibbs-Duhem relation $G_i^E = [\partial(n_T G^E)/\partial n_i]_{T,p,n_j}$ and the Gibbs-Helmholtz relation $[\partial(G^E/T)/\partial T]_{p,X} = -H^E/T^2$. G^E is the excess free energy of mixing — that is, in excess of the ideal term $G_{mix}^I = RT \sum_i X_i \ln X_i$ — and H^E is the excess enthalpy. G_i^E is generally represented in terms of a physical model containing dependencies on all $X_j (j \neq i)$ and T , and adjustable parameters which characterize the interaction of a single species with all others in solution. Using laboratory measurements of the total pressure, temperature, and compositions of the liquid and vapor phases at equilibrium, the values of these parameters can be determined. The resulting model for vapor-liquid equilibrium can then conveniently and accurately be used to calculate pressures, compositions, condensation altitudes, and their dependencies on changing climatic conditions. A specific system being investigated in our work is $\text{CH}_4\text{-C}_2\text{H}_6\text{-N}_2$, at conditions relevant to Titan's surface and atmosphere. We discuss: the modeling of existing data on $\text{CH}_4\text{-N}_2$, with applications to the composition of Titan's condensate clouds; some new measurements on the $\text{CH}_4\text{-C}_2\text{H}_6$ binary, using a high-precision static/volumetric system, and on the $\text{C}_2\text{H}_6\text{-N}_2$ binary, using the volumetric system and a sensitive cryogenic flow calorimeter; and describe a new cryogenic phase-equilibrium vessel with which we are beginning a detailed, systematic study of the three constituent binaries and the ternary $\text{CH}_4\text{-C}_2\text{H}_6\text{-N}_2$ system at temperatures ranging from 80 to 105°K and pressures from 0.1 to 7 bar.

VOLATILES IN CRYOGENIC PLANETARY ENVIRONMENTS

From the Earth's orbit sunward, ambient temperatures are sufficiently high that only refractory (ionic, metallic, or polymeric) materials and compounds with strong intermolecular forces (for example, hydrogen bonds in sulfuric acid and water) condense to solid and liquid form. However, at many locations farther from the sun, the surface or atmospheric temperatures are sufficiently cold that more weakly associating polar and nonpolar molecules (dominated by van der Waals forces) constitute most of the volatiles, where by volatiles we mean compounds which have sufficient vapor pressure to be present in the gas, as well as the liquid and/or solid, states. These systems fall within the temperature regime referred to as cryogenic in laboratory research.

The solid-vapor equilibrium of CO_2 in the atmosphere and surface of Mars, of NH_3 in the atmospheres of Jupiter and Saturn, and of SO_2 on the surface of Io involve molecules of moderate bond polarities and temperatures ranging down to about 100°K . These examples form a transition to the truly nonpolar volatiles mostly participating in equilibria near and below 100°K : CH_4 , Ar, and perhaps N_2 , as components of cloud condensates on Uranus and Neptune; CH_4 , N_2 , and perhaps Ar, as components of both clouds and, with C_2H_6 and C_3H_8 , of surface liquid on Titan; and finally N_2 , CH_4 , and perhaps Ar, CO, or other species in solid-vapor equilibrium on the surfaces of Triton and Pluto.

The first goal of laboratory research on these species is to obtain a complete description of the vapor pressures, gas equations of state, and volumetric and thermodynamic characteristics of the compounds in their pure liquid and gaseous states, at temperatures and pressures relevant to planetary environments. Generally, published work at the low pressures p and temperatures T appropriate to these cryogenic planetary conditions tends to be sparse compared to that available at higher p and T . This problem is least serious for the pure components, for which good data is generally available.^(1,2) However, most (if not all) of the condensate-vapor equilibrium systems mentioned above involve more than one species, so that one needs to study in the laboratory, and accurately represent by empirical or theoretical models, the equilibria in binary and multicomponent systems as well.

This need is especially realized at Titan, where N_2 can form a substantial part of CH_4 condensate in the clouds, and a large inventory (about 700 m) of C_2H_6 and C_3H_8 expected from photochemistry virtually guarantees a liquid CH_4 - C_2H_6 - N_2 - C_3H_8 -... system at the surface, in equilibrium with the atmosphere. Present as minor solutes in the cloud and ocean will be other hydrocarbons and nitriles: the nine detected by Voyager and, on the basis of plasma chemistry studies,⁽³⁾ several others. These arrive from above in the

form of precipitating stratospheric condensates. Measuring and/or modeling the solubilities of these minor solutes is another relevant topic, but one which we do not address further here.

The major condensates and thermodynamic regimes relevant at Titan are summarized in Figure 1. We use the interesting examples of Titan's $\text{CH}_4\text{-N}_2$ clouds and N_2 -hydrocarbon multicomponent surface to illustrate the thermodynamic principles involved. We describe some of the techniques which can be applied to study experimentally, and accurately model, such systems. The focus of this paper reflects experimental work and modeling by W. Reid Thompson of Space Sciences at Cornell, Jorge Calado of the Technical University of Lisbon, Portugal, and John Zollweg of Chemical Engineering at Cornell, who, along with Chris McKay of NASA/Ames, are coinvestigators in a laboratory research project funded by the NASA Planetary Atmospheres Program.

LABORATORY DATA ON $\text{N}_2\text{-(Ar)-HYDROCARBON}$ SYSTEMS

Due in part to their engineering importance, N_2 , CH_4 , C_2H_6 , and C_3H_8 are well-characterized in the pure state. But for mixtures, the increased degrees of freedom which must be explored in the laboratory makes the availability of data covering all relevant $p\text{-}T\text{-}X$ space less likely. (X is the mol fraction of a component in the liquid.) Data at the relevant low temperatures and pressures are particularly sparse.

We summarize the available data for vapor-liquid equilibrium in binary and higher combinations of N_2 , CH_4 , C_2H_6 , C_3H_8 , and Ar in Table I. In order to accurately model the Titan clouds, one needs good data on the $\text{N}_2\text{-CH}_4$ system. This system is the best studied of the binaries, but available data does not guarantee consistent data.⁽⁴⁾ Most of the other binaries have few if any measurements at $T \leq 110^\circ\text{K}$, relevant to Titan's surface. In order to understand the vapor-liquid equilibrium (VLE) at Titan's surface, and form a working model of, for example, the thermal opacity—temperature—VLE feedback processes which are active on Titan, we must form a good working knowledge of the constituent binaries of the $\text{N}_2\text{-CH}_4\text{-C}_2\text{H}_6$ system, and preferably perform direct experiments on the $\text{N}_2\text{-CH}_4\text{-C}_2\text{H}_6$ ternary relevant to surface-atmosphere equilibrium. After some discussion of the basic thermodynamics and models, we describe two existing types of experimental apparatus with which we are better characterizing the $\text{N}_2\text{-C}_2\text{H}_6$ and $\text{CH}_4\text{-C}_2\text{H}_6$ binaries, and a third apparatus with which we can perform direct vapor-liquid composition measurements of multicomponent systems.

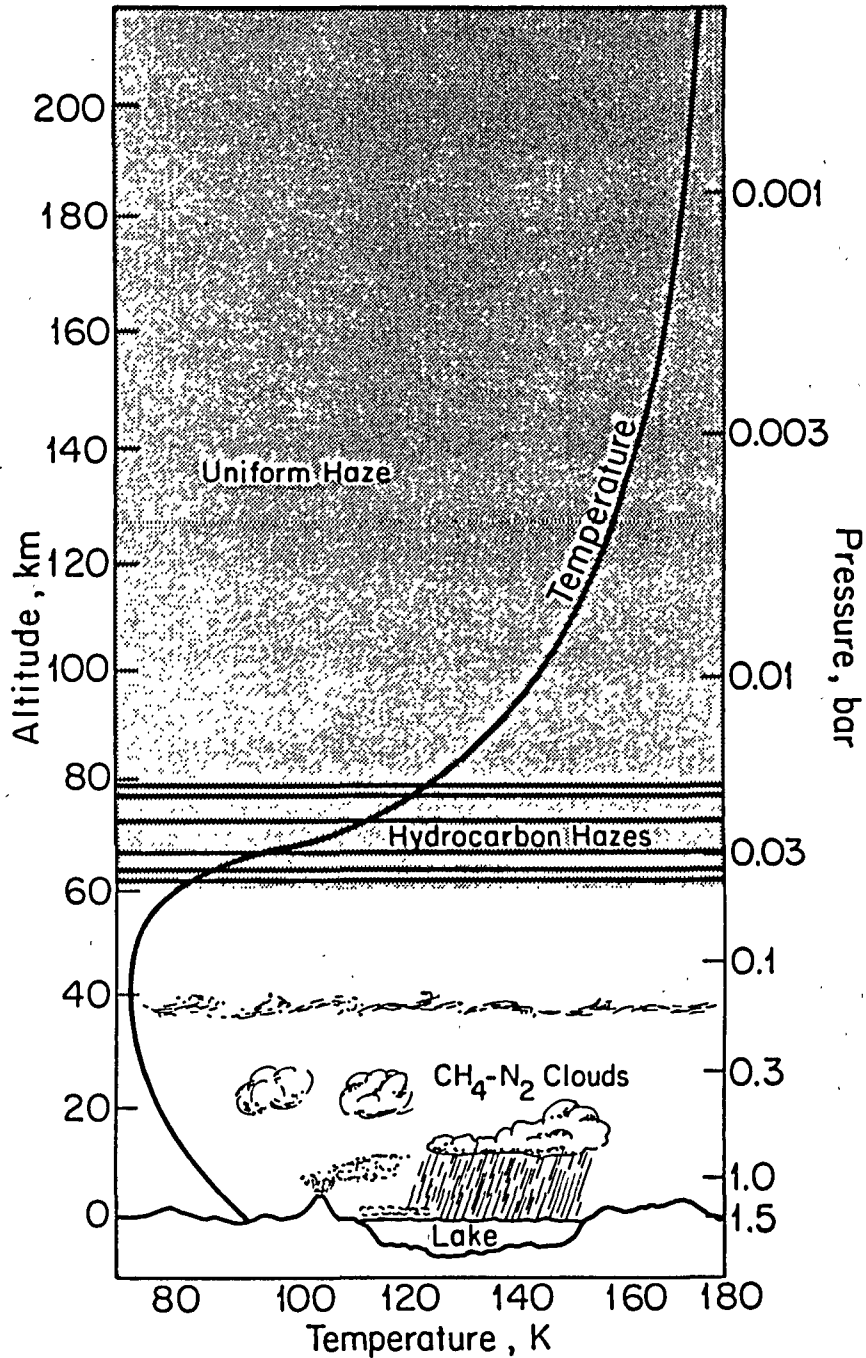


Figure 1. A sketch of Titan's atmosphere, surface, and condensates. A thick haze extends high into the stratosphere, while organic gases condense near the base of the stratosphere. Various types of $\text{CH}_4\text{-N}_2$ clouds are shown in the troposphere. There is evidence for precipitating clouds of $\text{CH}_4\text{-N}_2$ and surface lakes or oceans of $\text{C}_2\text{H}_6\text{-CH}_4\text{-N}_2\text{-...}$, as shown. The suggestion of geologic activity is artistic speculation only.

Table I

Availability of Experimental Data,
N₂-Ar-Hydrocarbon Systems

System	(<i>p, T</i>) Coverage	Assessment and Comments
N ₂ -CH ₄	$T \geq 91^\circ\text{K}$ $p \geq 0.2 \text{ bar}$	Fair coverage of (<i>p, T</i>) relevant to surface-atmosphere equilibrium if several studies are combined (about 20 <i>p, T, X</i> measurements total). Data applicable to atmosphere-cloud equilibrium more limited, with only a few measurements down to 80°K (cf. review of Kidnay <i>et al.</i> ⁽⁴⁾) <i>New modeling discussed here.</i>
Ar-CH ₄	$T \geq 92^\circ\text{K}$ $p \geq 0.16 \text{ bar};$ $T \geq 105^\circ\text{K}$ $p \geq 1.8 \text{ bar}$	Six points below 92°K (ref. 5). Adequate coverage above 105°K (refs. 6, 7). Poor below 105°K and for low <i>p</i> relevant to small Ar abundances expected.
N ₂ -Ar-CH ₄	$T = 112^\circ\text{K}$ $p \geq 3.0 \text{ bar}$	Limited to one temperature. ⁽⁸⁾ At <i>T</i> this high, low pressures correspond to Ar-dominated gas.
CH ₄ -C ₂ H ₆	$T \geq 111^\circ\text{K}$ $p \gtrsim 0.1 \text{ bar}$	Good coverage above 111°K, cf. review by Hiza, Miller and Kidnay. ⁽⁹⁾ Needs extension down to 91°K or even lower (eutectic at 72.5°K). <i>New work and modeling discussed here.</i>
N ₂ -C ₂ H ₆	$T = 110.9^\circ\text{K}$ $p \gtrsim 0 \text{ bar};$ $T \geq 101^\circ\text{K}$ $p \geq 6.9 \text{ bar}$	Useful data at 110.9°K (ref. 10); range of <i>T</i> only at high pressures. ⁽¹¹⁾ Need coverage at lower (<i>p, T</i>). <i>New work and modeling discussed here.</i>
N ₂ -CH ₄ -C ₂ H ₆	$T \geq 144^\circ\text{K}$ $p \geq 68.9 \text{ bar};$ $T \geq 171^\circ\text{K}$ $p \geq 1.9 \text{ bar}$	Available data ^(12,13) only at (<i>T, p</i>) much different than found on Titan. Three-phase (<i>ℓ - ℓ - v</i>) data exists for $T \geq 117^\circ\text{K}$, $p \geq 14 \text{ bar}$ (ref. 14). This most relevant ternary system needs study in the two-phase (<i>ℓ - v</i>) region to 90°K and lower.
CH ₄ -C ₃ H ₈	$T \geq 90^\circ\text{K}$ $p \gtrsim 0.01 \text{ bar}$	Good coverage above 90°K, cf. review by Miller, Kidnay and Hiza. ⁽¹⁵⁾ Study could be extended to lower <i>T</i> , toward eutectic.
N ₂ -CH ₄ -C ₃ H ₈	$T \geq 114^\circ\text{K}$ $p \geq 2.9 \text{ bar}$	Fair coverage above 114°K (ref. 16). Also three-phase (<i>ℓ - ℓ - v</i>) data for $T \geq 117^\circ\text{K}$, $p \geq 13.8 \text{ bar}$ (ref. 14).
Ar-CH ₄ -C ₂ H ₆	$T = 116^\circ\text{K}$ $p \geq 4.0 \text{ bar}$	Limited to one temperature and relatively high pressures. ⁽¹⁷⁾
CH ₄ -C ₂ H ₆ -C ₃ H ₈	$T \geq 115^\circ\text{K}$ $p = 1.0 \text{ bar}$	Some useful data. ⁽¹⁸⁾ Needs study at lower (<i>p, T</i>).
N ₂ -Ar-C ₂ H ₆ , etc.	—	Other relevant systems not studied, or at much higher (<i>p, T</i>) than relevant for Titan.

CONDENSATE-VAPOR THERMODYNAMICS OF MIXED SYSTEMS

For the simple case of an ideal solution, the pressure of a component p_i is simply proportional to its mol fraction X_i in the liquid. The statement of Raoult's law, and the free energy of mixing for an ideal solution, are

$$p_i = X_i p_i^o$$

$$G_{mix}^I = RT \sum_i X_i \ln X_i \quad (1)$$

where p_i^o is the vapor pressure of i in the pure state, G_{mix}^I is the Gibbs free energy of mixing in the ideal case, and R is the universal gas constant.

For molecules with similar polarizabilities and sizes, Raoult's law can provide a reasonable first guess, but real systems always show some deviation from ideality. To characterize the thermodynamic behavior of real systems, the concept of excess quantities is introduced. An excess quantity is simply the *actual* measurement for a mixture minus that which would apply for the hypothetical *ideal* mixture. A pivotal quantity is the excess free energy

$$G^E = \sum_i X_i \mu_i^E \quad (2)$$

where μ_i^E is the chemical potential for species i ,

$$\mu_i^E = RT \ln \gamma_i \quad (3)$$

and γ_i is the *activity coefficient*. For calculating equilibria an expression for γ_i is central, since the general expression for the vapor pressure in a mixture is

$$p_i = \gamma_i X_i p_i^o \quad (4)$$

[Here, to facilitate readability, we write pressures p_i , implicitly assuming that the gases are ideal. In the real case, gases near their condensation temperatures are nonideal, and pressures are replaced by fugacities f_i . See Prausnitz *et al.*⁽¹⁹⁾ for a good description of the details.]

Several empirical, semi-empirical, and theoretical approaches can be followed to develop a mathematical or computational model for G^E . The usual approach is to adopt a mathematical representation for G^E , and obtain the expression for activity coefficients via the Gibbs-Duhem relation

$$\mu_i^E = RT \ln \gamma_i = \frac{\partial}{\partial n_i} \left[n_T G^E \right]_{T,p,n_j} \quad (5)$$

where n_i is the mols of component i and $n_T = \sum n_i$.

In developing a model, it is possible to perform a power-series expansion in (for the binary case) $(X_1 - X_2)$, or to formulate a model assuming that nonideality results mostly from enthalpic effects, or one which is dominated by entropic effects. At this time we do not consider the details of these models, but proceed to ask how one can pragmatically extract the needed information, and present examples of some accurate approaches and checks for consistency.

METHODS OF OBTAINING AND EVALUATING VLE DATA

First-order approximations can be obtained from Raoult's law, where for the ideal solution $\gamma_i \equiv 1$, or from Henry's law, a good approximation for gases far above their condensation T 's: $X_i = p_i/K_H$, where K_H is the Henry constant, $K_H = \lim_{X_i \rightarrow 0} \gamma_i p_i^0$. For rough calculations, this suffices for the CH_4 - N_2 system, where CH_4 is approximately ideal and N_2 approximately follows Henry's law. However, for accurate results the system must be modeled in a more general way. This is illustrated in Figure 2, where we show the degree of nonideality of CH_4 and N_2 under Titan conditions.

Another simple approach useful in some cases would be to simply extrapolate experimental data. This can to some degree be done for the CH_4 - N_2 system, but the data are seldom sampled in a uniform way, coverage of parameter space is limited, and Table 1 shows that little data is available for the other important systems. Generally, then, we need to formulate a model for the system, fit limited experimental data to that model, then use the model to compute the required quantities. As theoretical work progresses, it is also possible to predict some thermodynamic quantities and use them as a check on certain experimental quantities. Specifically, we may (1) experimentally measure the complete equilibrium by determining X_i and p_i for all components at a number of T 's; (2) experimentally measure only X_i and total pressure p_T , which is sufficient if an explicit form for G^E is adopted; (3) determine the form of G^E from thermodynamically related measurements, such as calorimetry; or (4) rely on theoretical calculations, at least in part.

Empirical Modeling of X_i, p_i Measurements

First we discuss the CH_4 - N_2 system, and demonstrate that both the compositional and temperature dependence of the nonideality can be well modeled by a form beginning from theory but modified empirically. We use the data of Parrish and Hiza⁽²⁰⁾ from 95 to 120°K, and of McClure *et al.*⁽²¹⁾ for 90.68°K. It will turn out that these data are very consistent within the eventual adopted model.

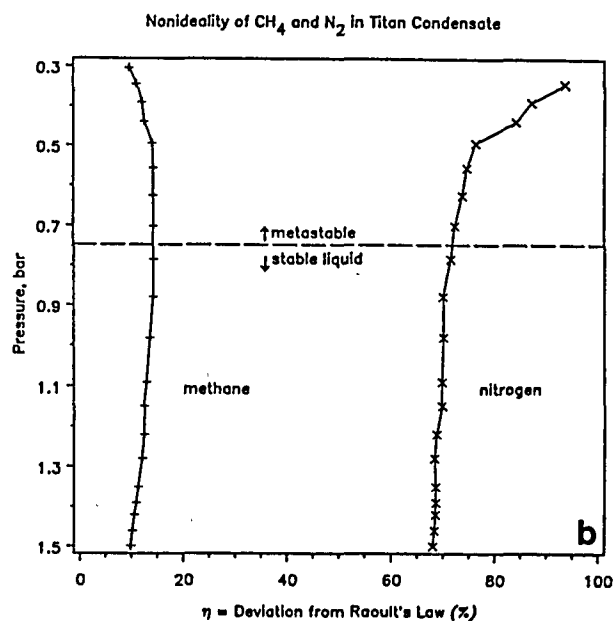
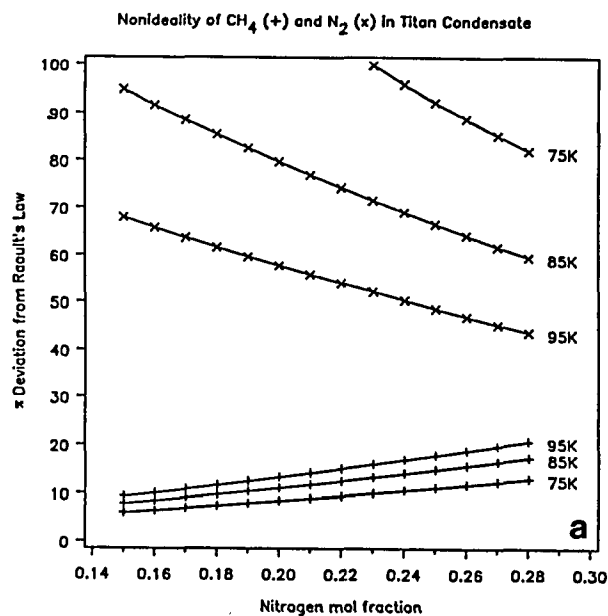


Figure 2. (a) Nonideality $\eta \equiv \gamma - 1$ of CH_4 and N_2 in binary solutions over temperatures and mol fractions spanning ranges appropriate to Titan's troposphere. The deviation from ideality (from Raoult's law) for CH_4 is about 10–15% and shows some concentration and temperature dependence. For N_2 it is much larger; also, the strong, nonlinear compositional dependence indicates that a Henry's law approximation would be inaccurate. (b) Nonideality η of CH_4 and N_2 in Titan tropospheric cloud, for condensate computed to be in thermodynamic equilibrium with the atmosphere. The (p, T) conditions⁽²³⁾ vary from about $p = 1.5$ bar, $T = 94^\circ\text{K}$ near the surface to $p = 0.30$ bar, $T = 73.5^\circ\text{K}$ at the highest altitude where condensation is computed to occur. These plots pertain to liquid CH_4 - N_2 condensate, which is metastable (with respect to solid solutions) above the indicated level.

The first exercise was to model the data with the same simple regular-solution form previously used by Thompson,⁽²²⁾

$$RT \ln \gamma_i = \sum_{j \neq i} \alpha_{ij} X_j^2, \text{ or}$$

$$\gamma_i = \exp[(1/T) (\sum_{j \neq i} a_{ij} X_j^2)], \quad (6)$$

where R has been absorbed into the parameter a . This is equivalent to the first term of a Redlich-Kister expansion, which will be presented later. In this modeling, the activity coefficients were computed directly from the VLE data of Parrish and Hiza⁽²⁰⁾ by $\gamma_i = p_i/(X_i p_i^0)$. Letting subscript 1 denote CH₄ and 2 denote N₂, these fits yielded values $a_{1,2} = 156.5 \pm 4.5$ (γ_1 residual 0.0770) and $a_{2,1} = 53.1 \pm 1.6$ (γ_2 residual 0.0024). In Figure 3 we show the residuals, which are largest for CH₄ in N₂-rich mixtures and, although a much better fit overall, also large for N₂ in CH₄-rich mixtures. The arcing of the residuals indicates a need for more complex terms in (X_i, X_j) in the model equation. Even more noticeable are the trends with varying T , which cannot be removed just by adding those terms: a generalization of the T dependence is indicated.

Substantial experimentation with equations leads to a fairly simple form that describes the data very well, and is therefore useful as a model for calculations of vapor-cloud equilibrium on Titan. The form

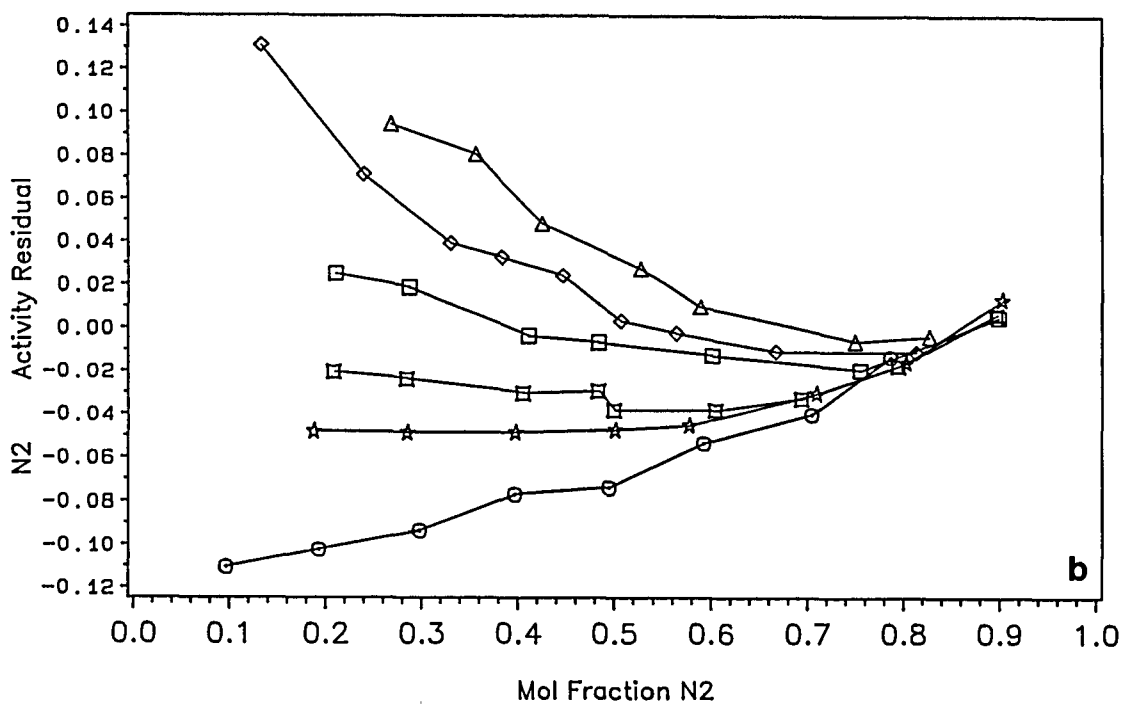
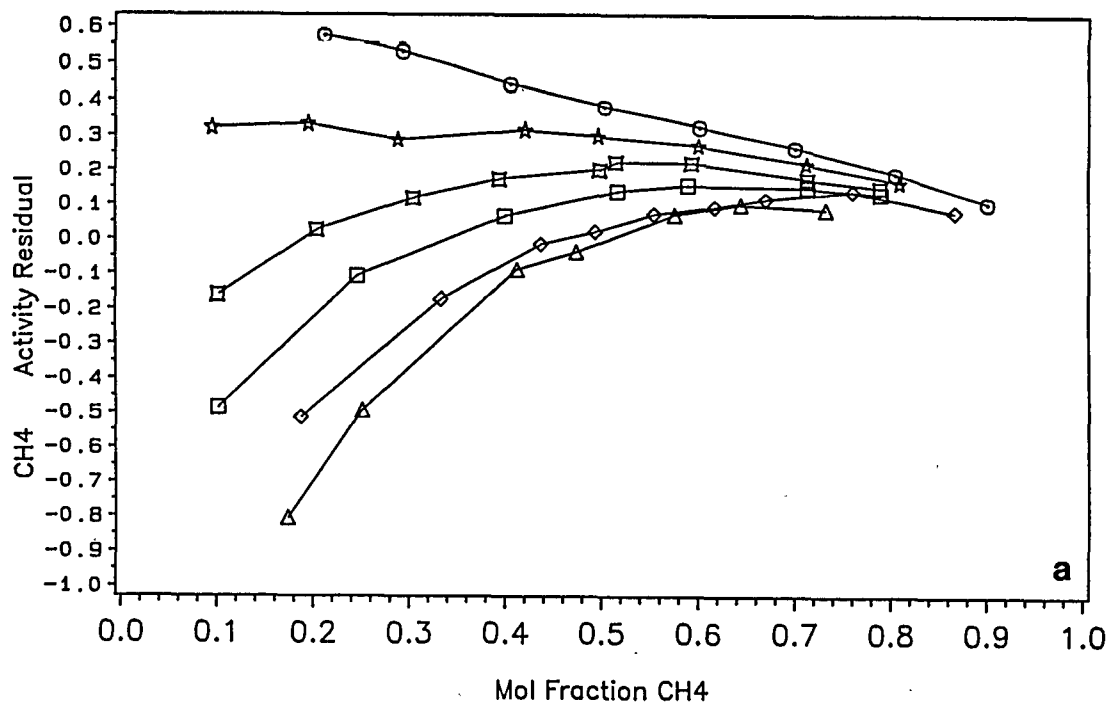
$$\ln \gamma_i = (b_i + c_i/T)[X_j^2 + q_i(X_i - X_j)X_j] \quad (7)$$

when fit to the 90.68°K data of McClure *et al.*⁽²¹⁾ with the 95, 100, and 105°K data of Parrish and Hiza⁽²⁰⁾ yields the fits shown in Table II.

Table II
Least-Squares Coefficients for N₂ and CH₄
Activity Coefficient Expressions

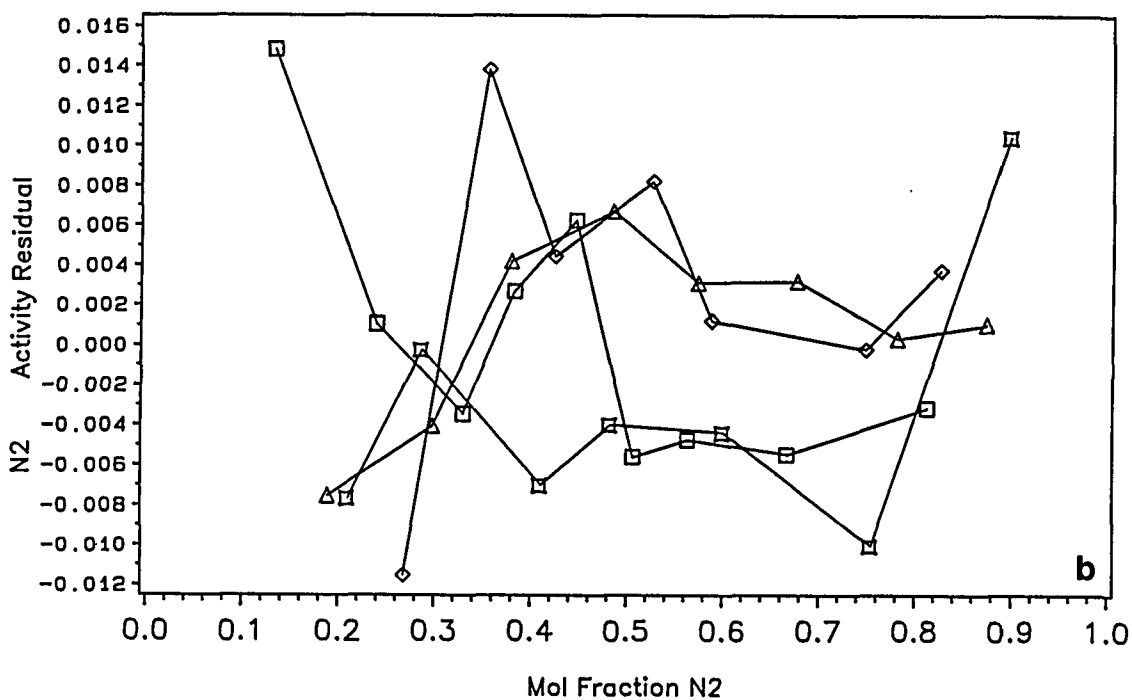
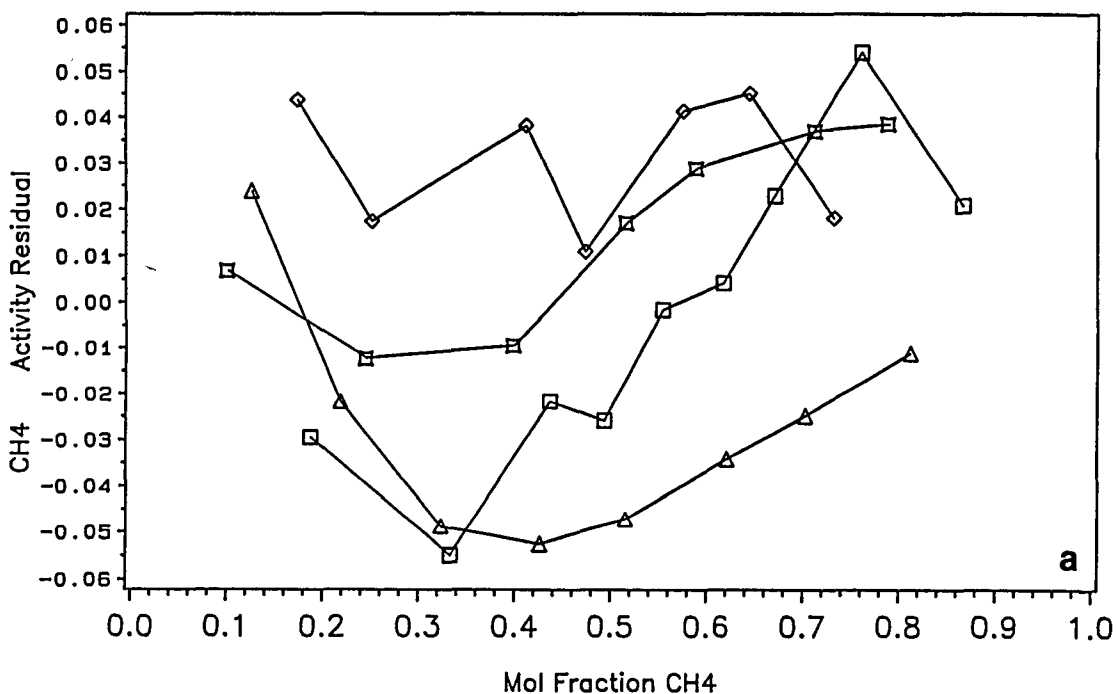
i	b_i	c_i	q_i	σ
N ₂	-0.935 ± 0.041	150.2 ± 4.0	-0.133 ± 0.013	4.3×10^{-5}
CH ₄	3.773 ± 0.131	-204.3 ± 12.2	0.307 ± 0.011	1.1×10^{-3}

From Figure 4 we see that any remaining systematic trends are very small. This model can be used to compute the composition of cloud droplets in Titan's atmosphere to high accuracy. (Note that in this case, nonideality of the gases has been absorbed into the model. While this simplifies calculations for the present application, an analysis separating the two effects, and considering other types of models, will be published elsewhere.)



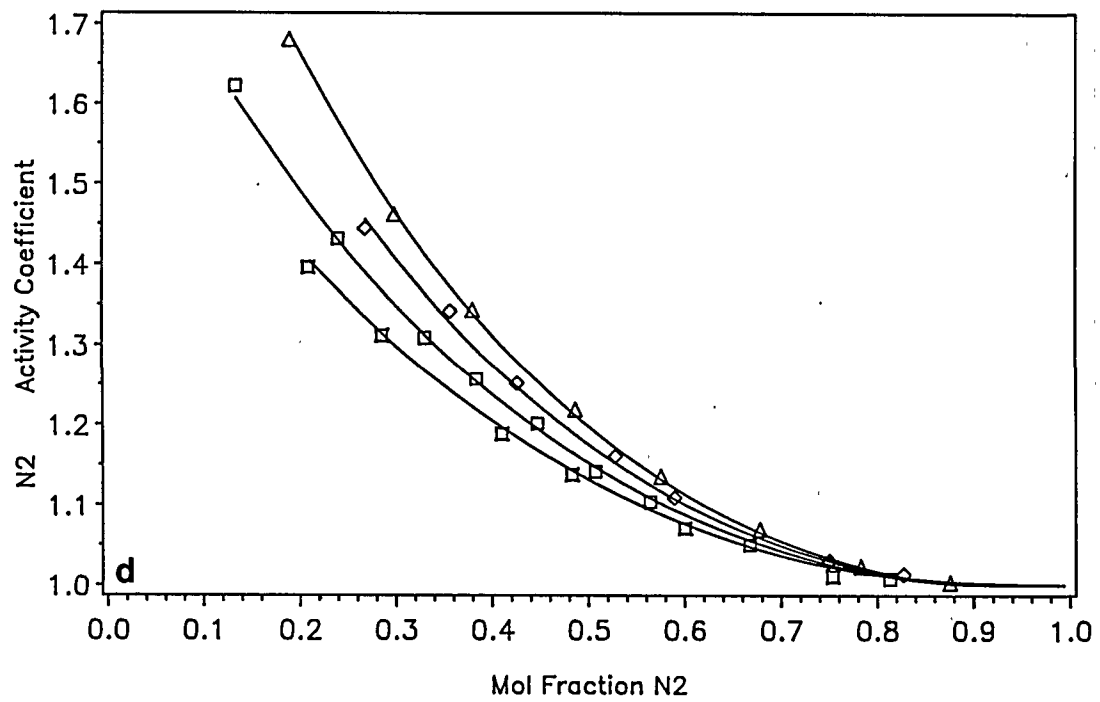
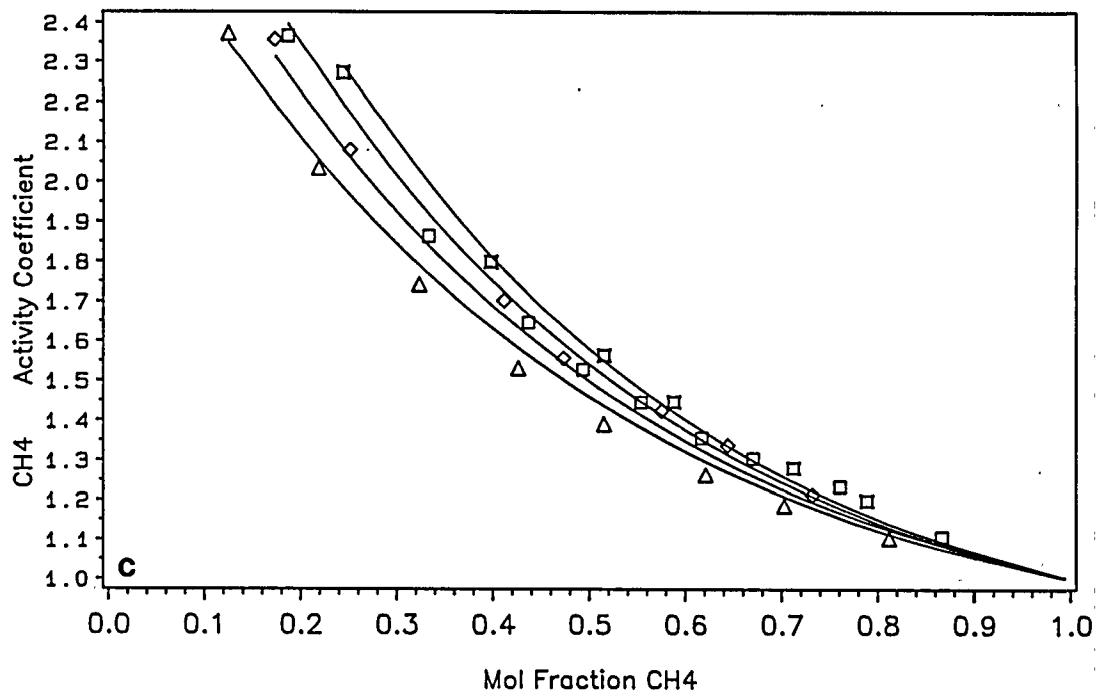
T_K ▲-▲-▲ 95 ◆-◆-◆ 100 □-□-□ 105 ▣-▣-▣ 110 ★-★-★ 115 ○-○-○ 120

Figure 3. Residuals for fits of the experimental CH₄-N₂ VLE data of Parrish and Hiza⁽²⁰⁾ to simple activity coefficient expressions $\ln \gamma_i = a_i X_j^2 / T$. Large deviations (especially for CH₄) and regular trends in the residuals indicate that a more complex expression is needed.



T_K $\triangle-\triangle$ 90.68 $\diamond-\diamond$ 95 $\square-\square$ 100 $\times-\times$ 105

Figure 4. Residuals (a,b) for fits of the experimental $\text{CH}_4\text{-N}_2$ VLE data of McClure *et al.*⁽²¹⁾ at 90.68°K and Parrish and Hiza⁽²⁰⁾ at 95, 100, and 105°K to a more complex empirical expression, $\ln \gamma_i = (b_i + c_i/T)(X_j^2 + q_i(X_i - X_j)X_j)$. Residuals are small, and systematic trends in the residuals are nearly eliminated. The derived parameters (Table II) in the above form provide an accurate basis for vapor-liquid equilibrium calculations.



T_K Δ Δ Δ 90.68 ◇ ◇ ◇ 95 □ □ □ 100 □ □ □ 105

Figure 4 (continued). Experimental points and the fitted function (solid lines) are plotted in (c,d).

We proceed to use the model to compute the composition of cloud droplets as a function of altitude in Titan's atmosphere. The physical process envisioned is the lifting of a parcel of $N_2 + CH_4$ gas from Titan's surface, checking for condensation at each level. CH_4 does not simply condense when its partial pressure exceeds the vapor pressure. Rather, in this binary system, condensation occurs when the chemical potential of the gas is greater than that of the equilibrium liquid. This is equivalent to having the sum of the CH_4 and N_2 mol fractions computed for the liquid (given the gas composition, p_T , and T) exceed unity. Every calculation of liquid composition requires an iterative solution, and if condensation occurs, calculation of the self-consistent liquid and (new) gas compositions (constrained by p_T) requires two coupled iterations. [The author can provide a computer program, or see ref. (19) for the strategies and some general implementations. We use the atmospheric structure of Lindal *et al.*⁽²³⁾ in these calculations.]

The results are shown in Table III and Figure 5. We begin with a large CH_4 gas-phase mol fraction $Y_{CH_4} = 0.14$ at the surface, so that the entire profile of composition can be seen. If the surface liquid is poor in C_2H_6 , condensation can begin close to the surface, and droplets of low-altitude fog will contain about 16% N_2 . Condensates at higher altitudes will have increasing N_2 abundances, at least through 12 km, where $X_{N_2} = 0.25$. Above that altitude, T falls below 82°K and freezing can begin. While the N_2 fraction in metastable liquid continues to increase, solubility in the solid is not as great, only about 15% at 14 km (81°K) [ref. (22)]. Droplets mixed vertically will partially degas 40% of their N_2 (about 10% of their total volume) upon freezing, no doubt producing distinctly shaped "sleet." At higher altitudes, the N_2 content of the solid condensate again increases as T decreases. Above 28 km, the T gradient becomes so low that no further condensation can take place in the CH_4 -depleted gas, which by now has only 2.0% CH_4 , whatever the abundance near the surface. Y_{CH_4} will remain at 2.0% to very high altitudes, where diffusive separation eventually causes it to rise again. The gas abundance of CH_4 and the composition and phase of the condensate are shown in Figure 6. There the radius of the outer circle is proportional to Y_{CH_4} , while the fractional area of the inner circle is proportional to X_{N_2} . A solid inner circle indicates solid condensate; in that case X_{N_2} is determined from the phase diagram shown by Thompson.⁽²²⁾

EXPANSION FORMS FOR G^E AND THERMODYNAMIC CONSISTENCY

Another approach to evaluating and modeling VLE data involves adopting an expansion form for G^E and recognizing that, given this form, liquid compositions and p_T alone (without gas compositions Y_i) can be used to determine the activity coefficients γ_i .

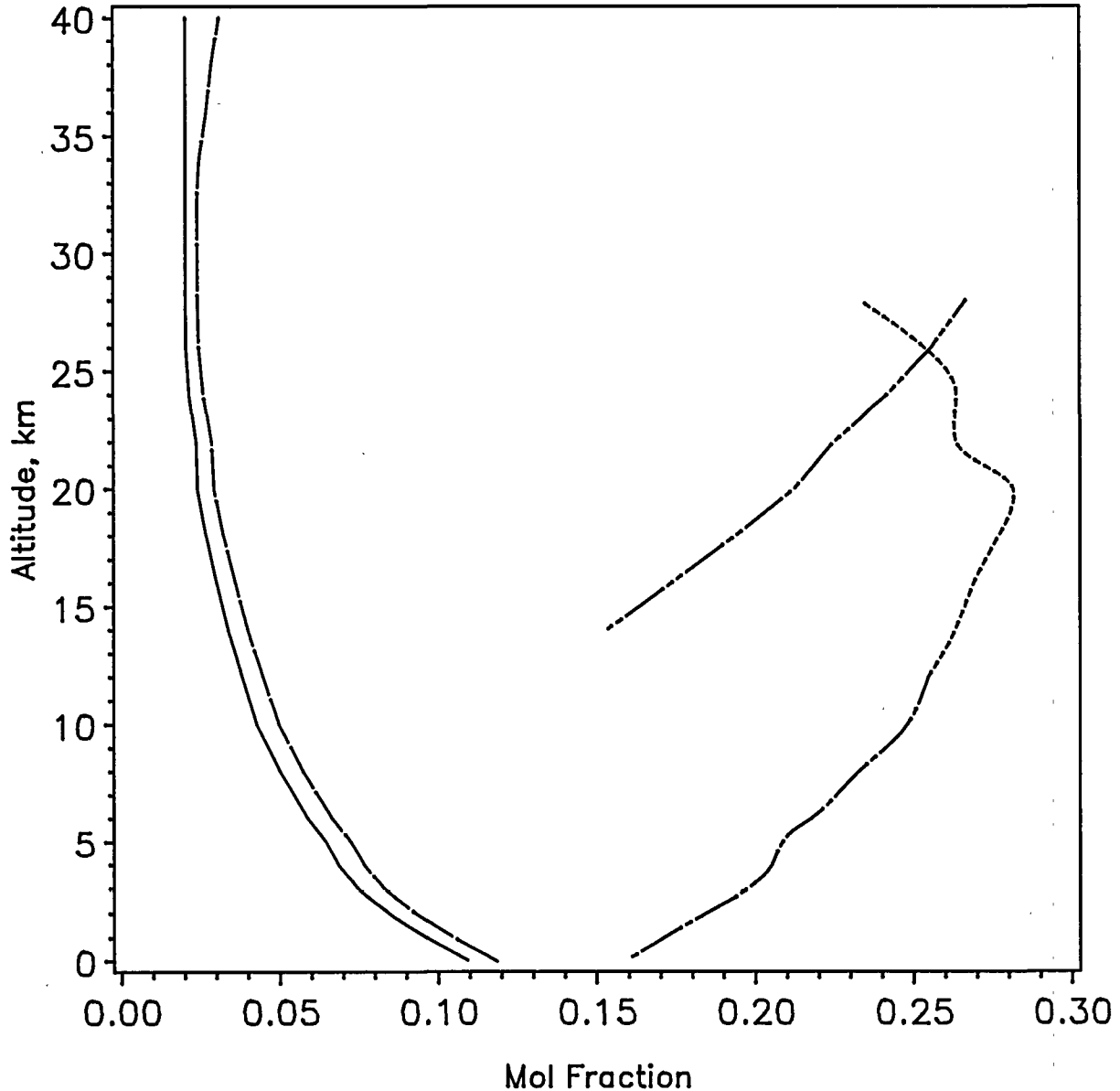


Figure 5. Computed equilibrium CH_4 and N_2 fractions in the gas and in liquid or solid CH_4 - N_2 condensate in Titan's troposphere. Here, the equilibrium compositions are computed for all altitudes. The actual lowest altitude where CH_4 + N_2 droplets can condense is determined by the CH_4 partial pressure at the surface, which is in turn determined by the C_2H_6 mol fraction in the ocean.⁽²²⁾ The solid line at left shows the actual saturation gas-phase mol fraction $Y_{\text{CH}_4}^{\text{sat}}$, while the accompanying dashed line shows the value $Y_{\text{CH}_4}^{\text{sat,pure}}$ which would apply if CH_4 condensed as the pure liquid. For the liquid, N_2 mol fractions are plotted at right. The long-short dashed line beginning at the surface gives X_{N_2} for liquid condensate. Its extension (short-dashed line) to higher altitudes shows X_{N_2} computed for the liquid, which is metastable with respect to solid at these altitudes ($T < 82^\circ\text{K}$). The double-dashed line gives the mol fraction of N_2 in solid condensate, which is also a CH_4 - N_2 solution.⁽²²⁾ Through most of the upper troposphere, the solubility of N_2 is less in the solid, which means that N_2 gas would exsolve upon freezing.

CH₄-N₂ Condensate Composition and Phase

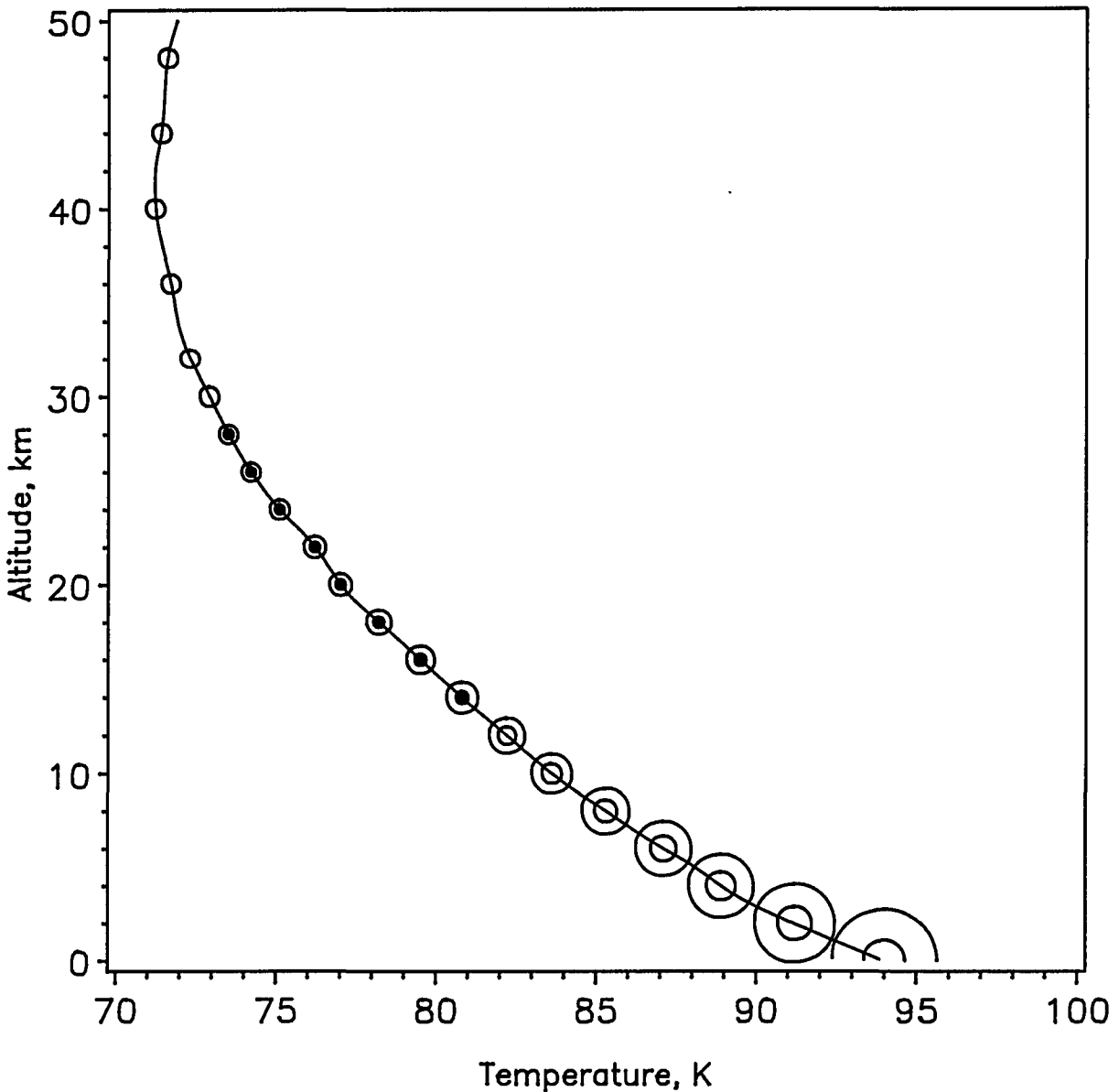


Figure 6. A nominal temperature profile for Titan's troposphere⁽²³⁾ is combined with the results of vapor-liquid equilibrium calculations for CH₄-N₂ (see Table III) to indicate the gas and condensate composition and phase. The radius of the outer circle drawn at selected altitudes is proportional to the true gas-saturation mol fraction $Y_{\text{CH}_4}^{\text{sat}}$, while the fractional area occupied by the inner circle equals the N₂ mol fraction in the liquid, X_{N_2} . Above 12 km, T falls below 82°K and the equilibrium phase of the condensate changes from liquid (open inner circles) to solid (solid inner circles). N₂ constitutes at least 15% and as much as 25% of the condensate particles, depending on altitude and condensate phase. Condensation does not occur above 28 km.

Table III
Vertical Profiles of Liquid-Vapor Equilibrium
in Titan's Troposphere

z , km	p , bar	T , °K	$p_{N_2}^o$, bar	$p_{CH_4}^o$, bar	$Y_{CH_4}^o$	p_{N_2} , bar	$p_{CH_4}^{sat}$, bar	$Y_{CH_4}^{sat}$	X_{CH_4}	γ_{N_2}	γ_{CH_4}
0.0	1.50	94.0	4.97	1.77E-1	0.1183	1.33	1.63E-1	0.1093	0.841	1.680	1.099
0.5	1.46	93.3	4.71	1.63E-1	0.1116	1.31	1.50E-1	0.1027	0.835	1.683	1.102
1.0	1.42	92.6	4.45	1.49E-1	0.1051	1.28	1.37E-1	0.0963	0.829	1.685	1.105
1.5	1.39	91.9	4.21	1.37E-1	0.0989	1.26	1.25E-1	0.0902	0.822	1.686	1.109
2.0	1.35	91.2	3.98	1.25E-1	0.0929	1.24	1.14E-1	0.0843	0.816	1.686	1.113
3.0	1.28	89.9	3.56	1.06E-1	0.0828	1.19	9.54E-2	0.0744	0.802	1.684	1.120
4.0	1.22	88.9	3.27	9.30E-2	0.0764	1.13	8.30E-2	0.0683	0.795	1.688	1.124
5.0	1.15	88.1	3.05	8.34E-2	0.0723	1.08	7.43E-2	0.0644	0.791	1.698	1.125
6.0	1.09	87.1	2.78	7.26E-2	0.0664	1.03	6.42E-2	0.0587	0.782	1.698	1.129
8.0	0.981	85.3	2.35	5.61E-2	0.0572	0.932	4.89E-2	0.0499	0.767	1.701	1.136
10.	0.879	83.6	1.99	4.35E-2	0.0495	0.841	3.74E-2	0.0425	0.752	1.700	1.142
12.	0.785	82.2	1.73	3.50E-2	0.0445	0.756	2.98E-2	0.0379	0.745	1.714	1.142
14.	0.701	80.8	1.49	2.79E-2	0.0397	0.678	2.35E-2	0.0335	0.737	1.724	1.143
16.	0.625	79.5	1.30	2.24E-2	0.0358	0.606	1.87E-2	0.0299	0.731	1.738	1.142
18.	0.556	78.2	1.12	1.78E-2	0.0321	0.541	1.48E-2	0.0265	0.723	1.746	1.142
20.	0.494	77.0	0.972	1.44E-2	0.0291	0.482	1.18E-2	0.0238	0.719	1.763	1.140
22.	0.438	76.2	0.883	1.24E-2	0.0283	0.428	1.03E-2	0.0234	0.737	1.841	1.125
24.	0.389	75.1	0.771	1.00E-2	0.0258	0.380	8.28E-3	0.0213	0.736	1.871	1.120
26.	0.344	74.2	0.687	8.41E-3	0.0244	0.337	6.97E-3	0.0203	0.747	1.936	1.110
28.	0.304	73.5	0.628	7.30E-3	0.0240	0.298	6.14E-3	0.0202	0.767	2.038	1.096
30.	0.269	72.9	0.579	6.45E-3	0.0240	0.264	5.42E-3	0.0202	—	—	—
32.	0.238	72.3	0.534	5.69E-3	0.0239	0.233	4.79E-3	0.0202	—	—	—
34.	0.210	71.9	0.506	5.22E-3	0.0249	0.206	4.23E-3	0.0202	—	—	—
36.	0.185	71.7	0.492	5.00E-3	0.0270	0.181	3.73E-3	0.0202	—	—	—
38.	0.163	71.4	0.472	4.69E-3	0.0287	0.160	3.30E-3	0.0202	—	—	—
40.	0.144	71.2	0.459	4.49E-3	0.0311	0.141	2.91E-3	0.0202	—	—	—

While there are many other analytic forms that can be developed for G^E , a useful general one is the Redlich-Kister expansion

$$\frac{G^E}{RT} = X_1 X_2 [a + b(X_1 - X_2) + c(X_1 - X_2)^2 + \dots] \quad (8).$$

Applying the Gibbs-Duhem relation and retaining three terms yields

$$\begin{aligned} \ln \gamma_1 &= \frac{X_2^2}{RT} [a - (1 - 4X_1)b + (1 - 8X_1 + 12X_1^2)c] \\ \ln \gamma_2 &= \frac{X_1^2}{RT} [a + (1 - 4X_2)b + (1 - 8X_2 + 12X_2^2)c] \end{aligned} \quad (9).$$

The parameters a , b , c , ... can be determined either by computing γ_i from X_i and p_i (as illustrated for CH_4 - N_2 above), and computing least-squares fits directly, or by using only X_i and p_T to achieve an iterative least-squares solution for the parameters.⁽²⁴⁾ In particular, this approach amounts to a least-squares solution to the equation

$$p_T = \exp\left[\frac{X_2^2}{RT}(a - b(1 - 4X_1) + \dots)\right] + \exp\left[\frac{X_1^2}{RT}(a + b(1 - 4X_2) + \dots)\right] \quad (10).$$

This method does not depend on Y_i measurements, which tend to be more uncertain than X_i measurements, and guarantees that p_T and X_i are consistent with the thermodynamic model.

Using this approach, data that seems inconsistent can sometimes be reevaluated. It has been applied to the data of Wilson⁽¹⁰⁾ for the $C_2H_6-N_2$ system, determining the values $a = 2.472$, $b = 0.479$ at 110.9°K. (Reevaluations and new measurements of $C_2H_6-N_2$ are due to coinvestigator J. Calado.) These parameters can be used to evaluate a quantity often used to intercompare data, $G_{X=0.5}^E$, which for $C_2H_6-N_2$ at 110.9°K is 570 J mol⁻¹. We report below some new measurements on this system.

EXPERIMENTAL TECHNIQUES

We describe techniques for obtaining vapor-liquid equilibria and relevant thermodynamic quantities for mixed systems in this section, giving examples corresponding to equipment which is being used in our investigations. The three systems can be described as total-pressure/volumetric, flow/calorimetric, and recirculation/liquid-vapor sampling systems.

Volumetric Total-Pressure System

In the all-glass volumetric VLE system at the Technical University of Lisbon, carefully measured quantities of gases are condensed into a pycnometer, which very accurately measures liquid volumes. Very stable T is achieved by using gases at their triple points as thermostats: CH_4 at 90.69°K and C_2H_4 at 103.99°K are particularly relevant for Titan studies. Measuring the total pressure and knowing the total composition and volumes allows an iterative calculation of the exact liquid and vapor compositions. Both VLE and liquid volumetric data are obtained. The experimental layout is shown in Figure 7; for more details, see ref. (25).

$C_2H_6-N_2$ experiment and theory.

Recent work with this system has provided new data on the $C_2H_6-N_2$ system at 90.69°K, which we summarize here. The $C_2H_6-N_2$ system shows only limited solubility, separating into two liquid phases over much of the compositional range. The miscibility gap extends from a maximum solubility of about 10–20% N_2 on the C_2H_6 -rich side to about 3–6% C_2H_6 on the N_2 -rich side. [See ref. (22) for a ternary phase diagram showing the miscibility limits for $C_2H_6-CH_4-N_2$ and (on its lower boundary) for $C_2H_6-N_2$; also see ref. (26) and below.]

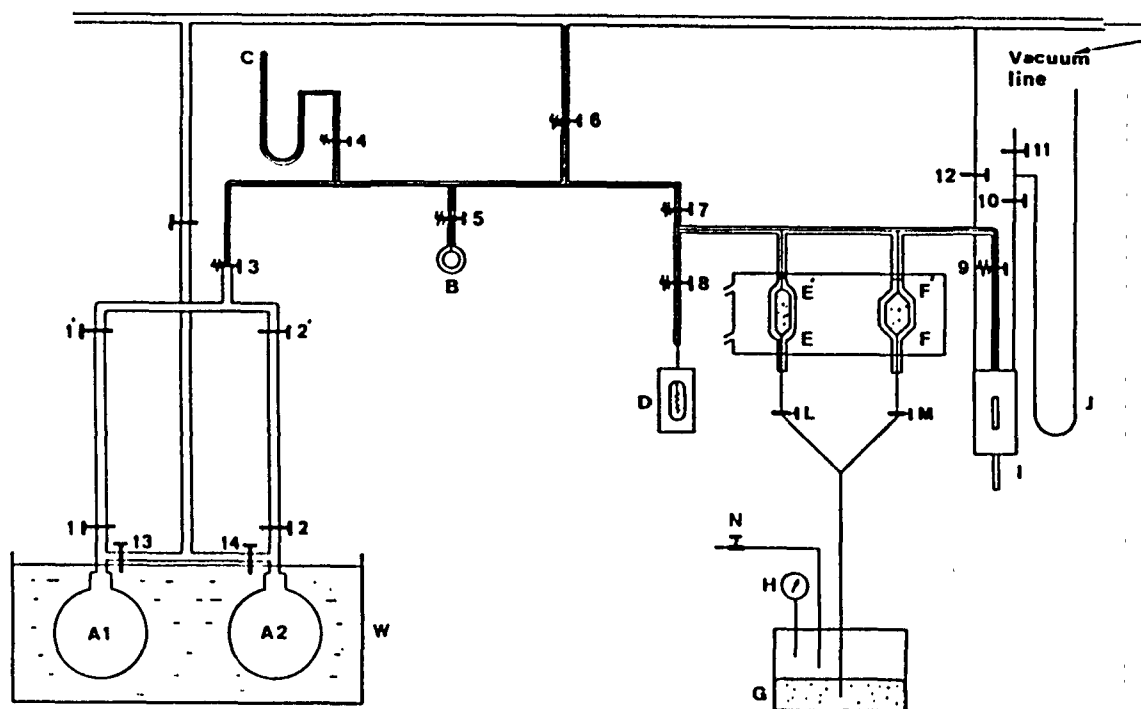


Figure 7. The low-to-moderate pressure, volumetric-manometric VLE system at the Technical University of Lisbon.⁽²⁵⁾ Thermostatted gas samples in A1-A2 are used to supply known quantities of two gases, which are condensed in the calibrated pyknometer (volumetric assembly) I. Once the gases are transferred, equilibrium is attained by expanding and contracting the vapor space using the volumes E and F, which can be filled either with vapor or with mercury from reservoir G. Knowing the initial composition, liquid volume, and total pressure provides data sufficient to compute G^E at a given temperature.

Details on the $C_2H_6-N_2$ system integrating data from several sources will be published elsewhere; however, we find the value of $G_{X=0.5}^E$ at $90.69^\circ K$ is $508.6 J mol^{-1}$. Using the Gibbs-Helmholtz relation

$$\left[\frac{\partial(G^E/T)}{\partial T} \right]_{p,X} = -\frac{H^E}{T^2} \quad (11)$$

gives a value for the enthalpy of mixing $H_{X=0.5}^E = 235 J mol^{-1}$. An absolute theoretical approach using the Kohler-Fischer perturbation theory and a WCA division of the intermolecular potential is also being pursued. N_2 and C_2H_6 molecules are modeled as hard spheres (1-center) or hard fused spheres (2-center). Results for calculations with both N_2 and C_2H_6 represented as 2-center fused spheres yield $G_{X=0.5}^E = 526 J mol^{-1}$, $H_{X=0.5}^E = 358 J mol^{-1}$, and $V_{X=0.5}^E = -1.74 cm^3 mol^{-1}$. [V^E is the excess volume, which can be estimated⁽²⁷⁾ to be $-1.89 cm^3 mol^{-1}$.] Comparison of these preliminary results with the experimental measurements shows good agreement for G^E and V^E , but indicates that the theory is too high or experiment is too low in estimating H^E .

CH₄-C₂H₆ studies.

Using this apparatus, the Lisbon investigators have also obtained new data on the CH₄-C₂H₆ system⁽²⁹⁾ at 90.69 and 103.99°K. In Figure 8 we show the variation of p_T (essentially, p_{CH_4}) with composition, and the departures from ideality in this system. In Figure 9 we show the complete thermodynamic profile of the system (G^E , H^E , and the computed excess entropy term TS^E versus composition). Combining the results of Miller and Staveley⁽²⁸⁾ for H^E at 91.5 and 112.0°K with the G^E relationships obtained from VLE at 90.69 and 103.99°K allows, through assumption of a Redlich-Kister form and integration of the Gibbs-Helmholtz equation, the derivation of T-dependent parameters:⁽²⁹⁾

$$a = 80.43/T + 0.4236 \ln T - 2.183$$

$$b = 29.65/T + 0.2405 \ln T - 1.300$$

$$c = 0.0432.$$

These may be used in eq. (9) to accurately describe the CH₄-C₂H₆ system at temperatures relevant to Titan.

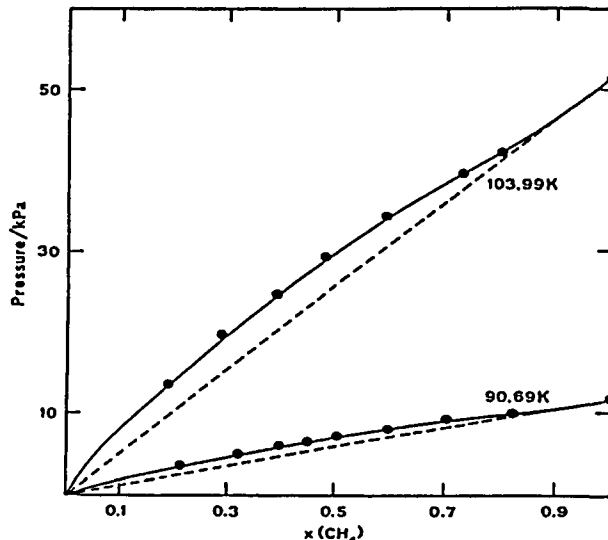


Figure 8. Experimental total vapor pressure versus composition for CH₄+C₂H₆ mixtures at 90.69°K and 103.99°K (ref. 29). Experimental data are solid dots joined by the smooth lines. Dashed lines represent the ideal state (Raoult's law).

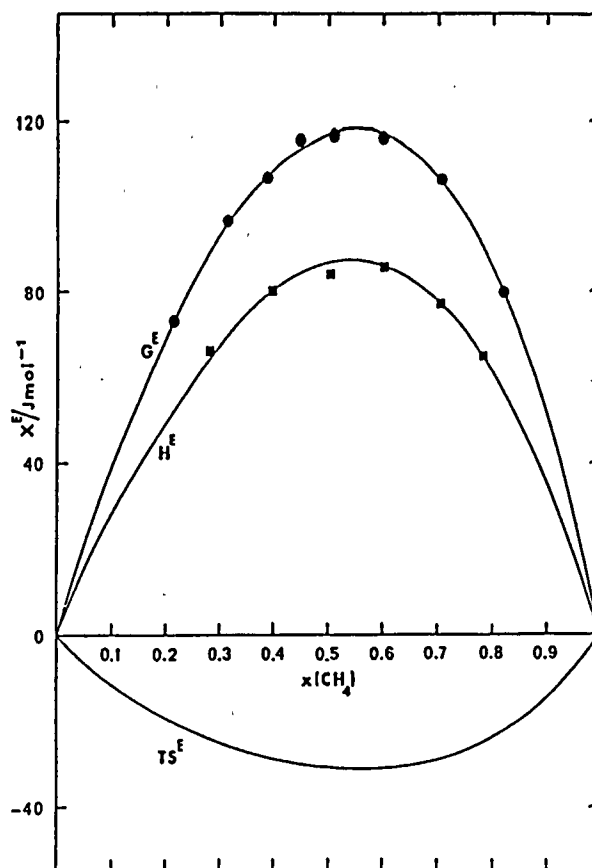


Figure 9. Excess thermodynamic quantities versus composition⁽²⁹⁾ for $\text{CH}_4\text{-C}_2\text{H}_6$ mixtures at $\sim 91^\circ\text{K}$. Excess free energy G^E is derived from fitting volumetric – total pressure results at 90.69°K to a Redlich-Kister equation, while enthalpy of mixing H^E is from calorimetric measurements at 91.5°K (ref. 28). The entropic term $TS^E = H^E - G^E$. Solid curves are computed from least-squares parameters determined for the Redlich-Kister equation.

Flow-Calorimeter System.

A second approach which can yield both direct thermodynamic measurements and, within the context of a model, parameters for VLE calculations is through calorimetric determinations of the heat of mixing H^E . In the School of Chemical Engineering at Cornell, our coinvestigator J. Zollweg and collaborators have developed a cryogenic, continuous-flow calorimeter,⁽³⁰⁾ a unique device for studying the H^E of liquefied gas binaries from 77 to 300°K and 0–150 bar. In this device (Figure 10), the basic principle is to compensate for the (generally) endothermic heat of mixing by supplying enough power to a heater in order to maintain a constant T in the calorimeter. The unit is computer controlled to monitor inlet, outlet, and calorimeter T 's, mass flow rates, and pressure; the computer also processes the data locally.

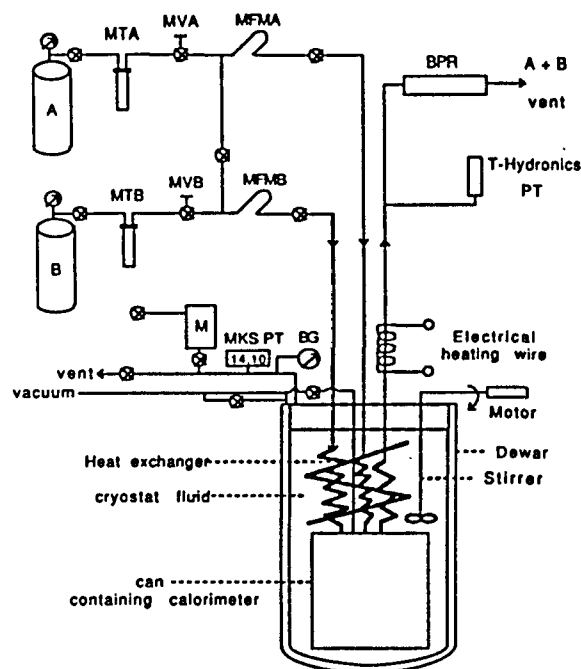


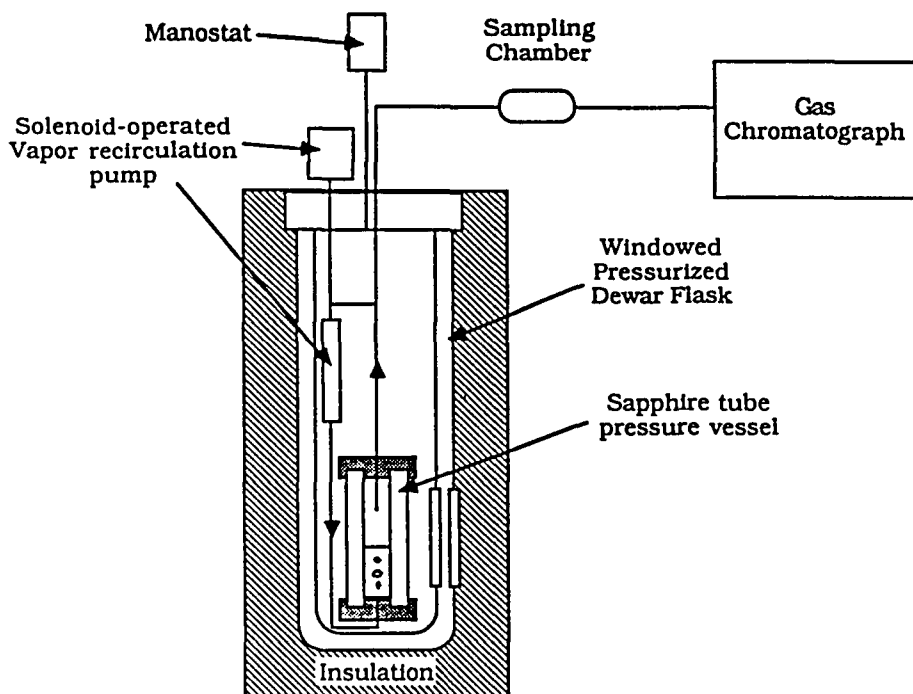
Figure 10. Schematic of the low temperature, high pressure flow calorimeter in the School of Chemical Engineering at Cornell University.⁽³⁰⁾ Continuous gas streams from A and B are metered, cooled, then mixed in the calorimeter. H^E is determined from the power required to maintain a constant temperature in the calorimeter, with other corrections. Abbreviations: MT: moisture trap; MV: metering valve; MFM: mass flow meter; PT: pressure transducer; BPR: back-pressure regulator; BG: Bourdon gauge; M: manostat.

We have used this unit to measure H^E for the $C_2H_6-N_2$ system at 92.3°K, both in the single-liquid-phase region and through the region of two liquid phases (the miscibility gap). The unusual ability to measure through the two-liquid region allows the miscibility limits to be defined more precisely. These results⁽²⁶⁾ have recently been reevaluated, yielding corrected values for the four points within the one-liquid region, shown in Table IV.

Table IV

Recomputed Heat-of-Mixing for $C_2H_6-N_2$ at 92.3°K

X_{N_2}	$H^E, J mol^{-1}$
0.1255	104.6
0.2145	150.2
...	...
0.9199	69.4
0.9706	21.5



Low Temperature Vapor-Liquid
Equilibrium Apparatus

Figure 11. Schematic illustrating the main components of the recirculating vapor, VLE system built recently in Space Sciences at Cornell University. Liquid is condensed into the central pressure vessel from external gas supplies (not shown), then vapor is recirculated using the pump to achieve rapid equilibrium. T is fixed by setting the pressure of the cryogenic fluid in the dewar (surrounding the pressure vessel) using a manostat. Two sample lines (one is shown) allow the withdrawal of both gas and liquid for precise compositional analysis using the gas chromatograph. Both binary and higher-order mixtures, specifically the $C_2H_6-CH_4-N_2$ system, can be studied with this apparatus.

Fitting this data to a regular solution form $H^E = aX_1X_2$ gives $a = 929$, so this work predicts $H_{x=0.5}^E = 232 \text{ J mol}^{-1}$, in good agreement with the value derived above from VLE data (235 J mol^{-1}).

Further work with constituent binaries of the $CH_4-C_2H_6-N_2$ system at a series of T 's is planned for this system. As shown above, adoption of a form for H^E and measurements of its variation with T allow the derivation of G^E through the Gibbs-Helmholtz equation. G^E in turn provides γ_i expressions through the Gibbs-Duhem equation.

Recirculating Vapor-Liquid Equilibrium System.

While the volumetric and calorimetric systems yield very useful data, we wish to obtain both a more thorough coverage of T -dependence for the CH_4-N_2 , $C_2H_6-N_2$, and $CH_4-C_2H_6$ binaries, and perform direct experiments on the $C_2H_6-CH_4-N_2$ ternary. For

this purpose, we have designed and built a cryogenic, recirculating, direct-sampling phase equilibrium vessel. A simplified schematic of this device is shown in Figure 11. It consists of a cylindrical sapphire tube pressure vessel, which has recirculating lines leaving the vapor space and reentering the liquid at the base. Vapor is actively pumped through this loop, so that equilibrium is achieved rapidly. Two sampling lines (one is shown) enter the top of the tube, and can be positioned to sample gas or liquid. Analysis of these samples by gas chromatography (GC) determines the mol fractions accurately and directly, independent of other volumetric or thermodynamic information. The tube is contained in a dewar with windows, so that the sample can be examined to allow tube positioning and to check for phase separation (two liquid layers) or of freezing. Temperature is selected by regulating the pressure of the cryostat fluid in the dewar, usually liquid N₂, with a manostat. Pressure is measured with a quartz-spiral Bourdon tube unit, and temperature with a platinum resistance thermometer. While the interior sample chamber is capable of high pressure, the operating pressure of this unit is intended to be 0–8 bar, 75–120°K, tailored to the many relevant measurements needed for Titan. Lower and higher T, p ranges can be realized with slight modifications. By incremental addition of the more volatile component, complete coverage of compositional ranges can be achieved fairly rapidly.

Our group of investigators has critically assessed and modeled experimental data on the CH₄-N₂, C₂H₆-N₂, and CH₄-C₂H₆ systems while building this unit, which is now undergoing final testing in the Space Sciences Building at Cornell. We will continue other studies while starting to obtain direct VLE measurements with this recirculating equilibrium system early in 1990. We welcome suggestions for experimental work, or technical inquiries about any of the three systems which we are using in this project.

ACKNOWLEDGMENTS.

Thanks to coinvestigator Jorge C. G. Calado for providing unpublished data and other material for the conference presentation. This work is supported by the NASA Planetary Atmospheres Program through grant NAGW-1444.

REFERENCES.

1. G. N. Brown, Jr. and W. T. Ziegler. *Adv. Cryogen. Eng.* **25** 662 (1980).
2. J. H. Dymond and E. B. Smith. *The Virial Coefficients of Pure Gases and Mixtures*. Clarendon, Oxford (1980).
3. W. R. Thompson, T. Henry, J. Schwartz, B. N. Khare and C. Sagan. *Center for Radiophysics and Space Research, Report 941*. CRSR, Cornell Univ., Ithaca NY (1989).

4. A. J. Kidnay, R. C. Miller, E. D. Sloan and M. J. Hiza. *J. Phys. Chem. Ref. Data* **14** 681 (1985).
5. H. Cheung and D. I.-J. Wang. *Indust. Eng. Chem. Fundam.* **3** 355 (1964).
6. D. Gravelle and B. C.-Y. Lu. *Can. J. Chem. Eng.* **49** 114 (1971).
7. A. G. Duncan and M. J. Hiza. *Indust. Eng. Chem. Fundam.* **11** 38 (1972).
8. R. C. Miller, A. J. Kidnay and M. J. Hiza. *J. Phys. Chem. Ref. Data* **9** 721 (1980).
9. M. J. Hiza, R. C. Miller and A. J. Kidnay. *J. Phys. Chem. Ref. Data* **8** 799 (1979).
10. G. M. Wilson. *Adv. Cryogen. Eng.* **20** 164 (1975).
11. A. T. Ellington, B. E. Eakin, J. D. Parent, D. C. Gami and O. T. Bloomer. In *Thermodynamic and Transport Properties of Gases, Liquids, and Solids*, p. 180. McGraw-Hill, New York (1959).
12. H. F. Cosway and D. L. Katz. *Amer. Inst. Chem. Eng. J.* **5** 46 (1959).
13. S.-D. Chang and B. C.-Y. Lu. *Chem. Eng. Progr. Symp. Ser.* **63** 13 (1967).
14. F. M. Llave, K. D. Luks and J. P. Kohn. *J. Chem. Eng. Data* **32** 14 (1987).
15. R. C. Miller, A. J. Kidnay and M. J. Hiza. *J. Phys. Chem. Ref. Data* **9** 721 (1980).
16. D. P. L. Poon and B. C.-Y. Lu. *Adv. Cryogen. Eng.* **19** 292 (1974).
17. I. M. Elshayal and B. C.-Y. Lu. *Cryogenics* **11** 285 (1971).
18. K. Watanabe, M. Kuroki, M. Ogura and I. Saito. *Cryogen. Eng. (Tokyo)* **4** 292 (1969).
19. J. M. Prausnitz, C. A. Eckert, R. V. Orye and J. P. O'Connell. *Computer Calculations for Multicomponent Vapor-Liquid Equilibria*. Prentice-Hall, Englewood Cliffs NJ (1967).
20. W. R. Parrish and M. J. Hiza. *Adv. Cryogen. Eng.* **19** 300 (1974).
21. D. W. McClure, K. L. Lewis, R. C. Miller and L. A. K. Staveley. *J. Chem. Thermodyn.* **8** 785 (1976).
22. W. R. Thompson. In *The Atmospheres of Saturn and Titan*, (ESA SP-241, Edited by E. Rolfe and B. Battrick), p. 109. ESA Public. Div., Noordwijk, Netherlands (1985).
23. G. F. Lindal, G. E. Wood, H. B. Hotz, D. N. Sweetnam, V. R. Eshleman and G. L. Tyler. *Icarus* **53** 348 (1983).
24. J. A. Barker. *Austral. J. Chem.* **6** 207 (1953).
25. J. C. G. Calado, E. J. S. Gomes de Azevedo, and V. A. M. Soares. *Chem. Eng. Commun.* **5** 149 (1980).
26. J. C. G. Calado, P. Gopal, J. A. Zollweg and W. R. Thompson. *Can. J. Chem.* **66** 626 (1988).
27. M. J. Hiza, W. M. Haynes and W. R. Parrish. *J. Chem. Thermodyn.* **9** 873 (1977).
28. R. C. Miller and L. A. K. Staveley. *Adv. Cryogen. Eng.* **21** 493 (1976).
29. E. J. S. Gomes de Azevedo and J. C. G. Calado. *Fluid Phase Equil.* (in press) (1989).
30. P. Gopal, J. A. Zollweg and W. B. Streett. *Rev. Sci. Instrum.* **60** 2720 (1989).